



Original article

The anti-invasive role of novel synthesized pyridazine hydrazide appended phenoxy acetic acid against neoplastic development targeting matrix metallo proteases



Yasser Hussein Eissa Mohammed^{a,c}, Prabhu Thirusangu^b, Zabiulla^a, Vigneshwaran V^b, Prabhakar B.T^b, Shaukath Ara Khanum^{a,*}

^a Department of Chemistry, Yuvaraja's College, University of Mysore, Mysore, 570005 Karnataka, India

^b Molecular Onco-medicine Laboratory, Postgraduate Department of Studies and Research in Biotechnology, Sahyadri Science College (A), Kuvempu University, Shivamogga, 577203, Karnataka, India

^c Department of Biochemistry, Faculty of Applied Science College, University of Hajjah, Yemen

ARTICLE INFO

Keywords:

Pyridazine
Metastasis
Dalton's lymphoma
MMPs
Cancer

ABSTRACT

Neoplastic metastasis is a major process where tumor cells migrate from the primary tumor and colonize at other parts of our body to form secondary tumor. Cancer incidences are rising and novel anti-neoplastic compounds with new mechanism of actions are essential for preventing cancer related deaths. In the current examination, a novel series of pyridazine analogues **6a-l** was synthesized and evaluated against metastatic neoplastic cells. Experimental data postulated compound **6j** has potential cytotoxic efficacy with prolonged activity against various cancer cells, including A549, HepG2, A498, CaSki and SiHa cells. Moreover, compound **6j** arrests the A549 migration and invasions markedly by counteracting matrix metalloproteinase (MMP)-2 and MMP-9 expressions. Also, compound **6j** proved its potentiality against Dalton's solid lymphoma progression *in-vivo* by abridging MVD and MMP expressions. Compound **6j** interacts with MMP-2 and MMP-9 by H-bond *in-silico*, thereby down regulates the MMPs action in tumourigenesis. Altogether, we concluded that compound **6j** down regulates MMP-2 and MMP-9 and thereby impairs metastatic cancer cell migration and invasions which can be translated into a potent anti-neoplastic agent.

1. Introduction

Cancer invasion and metastasis are pivotal events that renovate locally developing tumor into a systemic and life-threatening disease. Metastasis is a prime process where tumor cells spread from the primary tumor and colonize at distant organs to form secondary metastatic tumor and therefore, metastatic dissemination accounts for more than 90% of all cancer related deaths [1–4]. The cancer cells must migrate and invade through extracellular matrix (ECM), intravasate into the blood stream and lastly extravasate to form metastatic tumor [1,5,6]. In contrast to normal cells, cancer cells do not have physiological “termination signals” to stop the metastatic process [7–10].

Enhanced cell migration and invasion is an important hallmark of metastatic cancer cells. Hence, cancer cells degrade the ECM and basement membrane by overexpressing matrix metalloproteinases (MMPs) which allow the neoplastic cells to migrate and invade into the blood circulation for developing secondary tumor [5,6,8,10]. MMPs are engaged in executing a wide array of cellular and pathophysiological

functions including DNA transcriptional modifications, hematological pH regulation, elevating extracellular matrix digestion and many other functions *in vivo*. Taking into consideration, the importance of these pathophysiological functions, upregulation as well as deregulation of specific metallo proteases may play central role in several aspects of tumor development [11,12]. Most importantly, MMPs play a very crucial role in endothelial cell (EC) migration which facilitates the increased level of neovessel formation, aggressive tumor development and poor response to chemo and radiotherapies [5,6,10]. It is apparent that there is an urgency for innovative therapeutic strategies in the clinic to avoid metastatic spreading, hence, developing novel small molecules that specifically counteract tumor cell migration and invasion potency are critical for treatment of metastatic neoplasia.

Pharmaceutical science has initiated new era for the synthesis of plethora of organic molecules. Nitrogen-containing heterocyclic compounds have displayed various kinds of biological activities since a long time and increasing interest in the pharmaceutical science [13]. The pyridazine nucleus represents a versatile scaffold to develop new

* Corresponding author.

E-mail address: shaukathara@yahoo.co.in (S.A. Khanum).

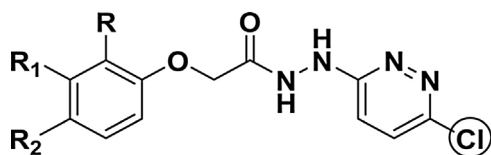


Fig. 1. Structure of *N'*-(6-chloropyridazin-3-yl)-2-phenoxyacetohydrazide analogues.

pharmacologically active compounds [14,15] that can be helpful in anti-microbial [16], anti-hypertensive [17], anti-cancer [18], anti-inflammatory [18,19] and anti-fungal activities [20]. This heterocyclic system has a broad range of biological activities and can also be used to link other pharmacophoric groups [20–24]. Pyridazine with other heterocyclic/pharmacophoral ring possess potential antitumor activity rather than pyridazine alone [25–28]. For instance, minaprine, which is used against depression nowadays, is a psychotropic drug. Numerous derivatives of 3-amino pyridazines also perform as specific GABA-A receptor antagonists. Not only Alzheimer's disease but also other neurodegenerative diseases like Parkinson's can be treated by therapeutic agents of pyridazines scaffold [29,30]. Extensive applications of pyridazine analogues have been found in the treatment of dermatosis, dry eye disorders and prostate cancer [31]. The diverse biological activity and promising anti-proliferative potency of pyridazine ring encouraged and prompted us not only to synthesize but also to validate a new series of 3-chloro-6-hydrazinylpyridazine analogues **6a-l**. In this endeavor, our efforts towards the design of new anti-cancer agents is considered to be worthwhile to pursue further modifications on the phenoxy acetic acid moiety by appending pyridazine hydrazide (Fig. 1) for inhibition of tumor cell proliferation of mouse and human origin. In the current investigation, we are focusing on the anti-neoplastic and invasive effect of pyridazine analogues by using *in-vitro*, *in-vivo* and *In-silico* assay systems.

2. Result and discussion

2.1. Chemistry

Synthesis of the target compounds, novel pyridazine analogues **6a-l**, was performed according to the reactions illustrated in Scheme 1. All the synthesized compounds were established by IR, proton NMR and mass spectral data. The commercially available substituted phenols, **1a-l**, were reacted with chloro ethyl acetate **2** in the presence of anhydrous potassium carbonate and acetone to afford phenoxy acetic ethyl esters **3a-l** which were hydrolyzed by treating with sodium hydroxide solution to provide the corresponding phenoxy acetic acid analogues **4a-l**. The corresponding final compounds, **6a-l**, were successfully synthesized by coupling compounds **4a-l** with 3-chloro-6-hydrazinylpyridazine **5b** using *O*-(benzotriazol-1-yl)-*N,N,N',N'*-tetra methyl uranium tetra fluoro borate (TBTU) as coupling agent, 2,6-lutidine as a base, and dichloromethane (DCM) as a solvent. All the structures of newly synthesized compounds were assigned on the basis of their spectroscopic data; IR, NMR, LC-MS and C, H, N analysis. The spectra of compound phenoxy acetic ethyl esters **3a** which were confirmed by the disappearance of the OH stretching of compounds **1a** and appearance of carbonyl stretching band for the ester group in the IR absorption spectra. The proton NMR observations of these compounds revealed that, broad singlet for the OH proton of compound **1a** disappeared and triplet and quartet for CH₃ and CH₂ protons respectively appeared. The spectra of compound 2-phenoxyacetic acid **4a** were considered as a representative example of the series **4a-l**. In IR spectra, the compound **4a** showed bands at 1751 and 3375 cm⁻¹ corresponding to carbonyl and OH stretching frequencies respectively. In ¹H NMR spectra of compound, **4a** showed one singlet at 4.69 assigned to OCH₂ protons. It also revealed multiplet signal in the range δ 6.96-7.31 for aromatic protons as well as singlet at 12.73 for OH proton. The mass spectra of compound **4a** gave significant stable M+ peak at *m/z* 152. Further,

spectra of the title compound **6a** was considered as a representative example of the series **6a-l**. The IR spectra of the compound **6a** was confirmed by the disappearance of the OH stretching and the appearance of two NH absorption peaks at 3120–3220 cm⁻¹. In addition, ¹H NMR spectra showed disappearance of OH proton at δ 12.73 and appearance of two NH protons and an increase in two aromatic protons with earlier aromatic proton peaks at δ 9.50, 10.30 and 6.92-7.65 respectively, which clearly affirmed the formation of compound **6a**. The mass spectra of compound **6a** gave significant stable peaks at *m/z* 279 (M +) and 281 (M + 2). Moreover, all the target compounds **6a-l** were clearly confirmed by ¹³C NMR.

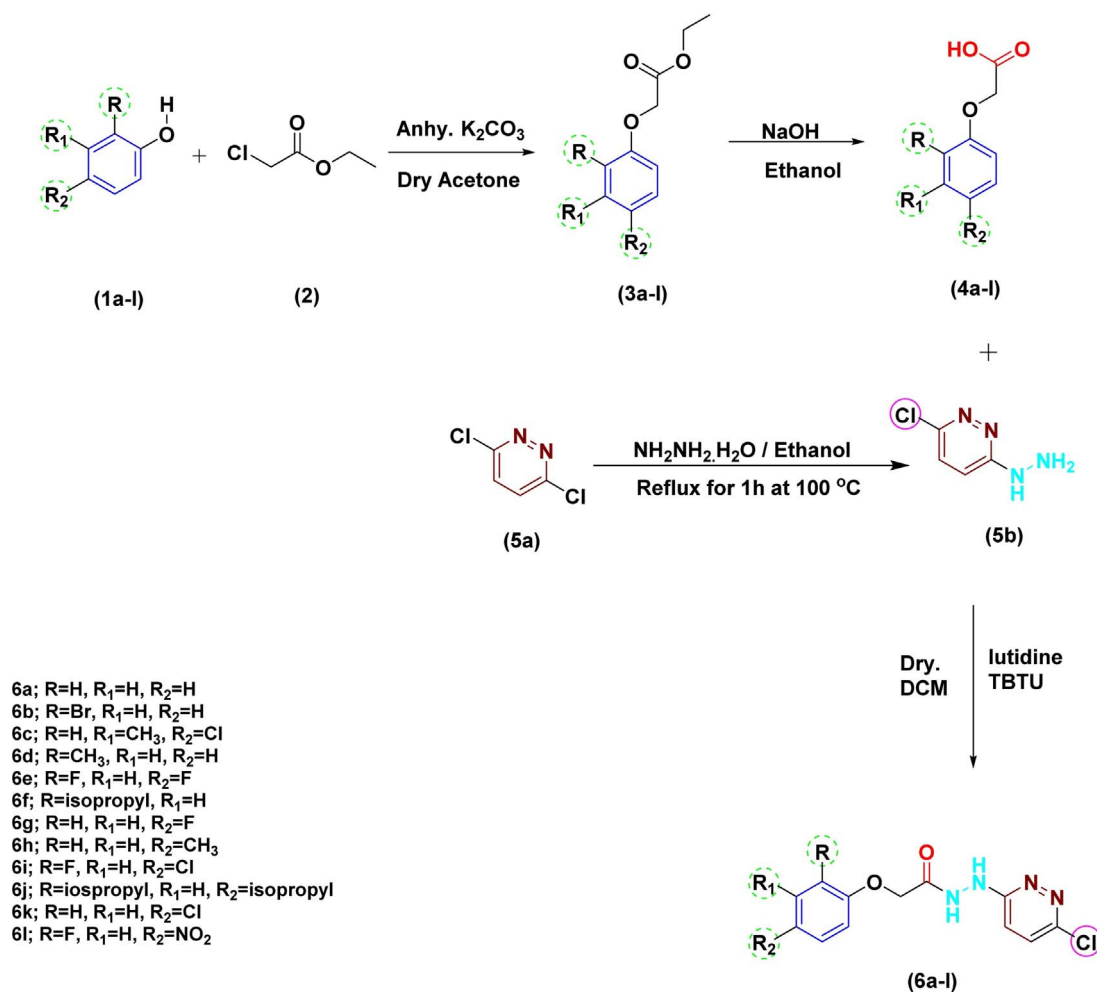
2.2. Biology

2.2.1. Cytotoxic effects of compounds **6a-l** against various invasive cancer cells

In the current scenario, cancer prevalence is increasing and there is a need for novel anti-neoplastic compounds with new mechanisms of actions for the prevention of cancer related death. In the recent period, synthetic active molecules have played an important role in the development of anticancer drugs with target specific action [2–4,28–31]. The pyridazine nucleus is a novel category of biologically/pharmacologically active moiety and also dimerized pyridazine with other moiety which has various potent pharmacological effects, including anti-cancer, anti-hypertensive, anti-inflammatory, anti-microbial and anti-fungal activities, than pyridazine alone [15–20,25–28]. In this investigation, a new series of pyridazine analogues **6a-l** was synthesized by incorporating CH₃, F, Cl, Br, H, NO₂ and isopropyl groups in the benzene ring, also cytotoxicity against A549, HepG2, A498, CaSki, SiHa and NIH-3T3 (normal fibroblast) cells were analyzed by MTT, trypan blue and LDH release assays. The average cytotoxicity of compounds **6a-l** was calculated against each cell line. Among the series, compound *N'*-(6-Chloropyridazin-3-yl)-2-(2,4-diisopropylphenoxy)acetohydrazide (**6j**) was found to exhibit a cytotoxic effect with IC₅₀ at 6.6 ± 0.6, 6.9 ± 0.7, 6.8 ± 0.8, 7.5 ± 0.5 & 7.8 ± 0.4 against A549, HepG2, A498, CaSki & SiHa cells, respectively and with very negligible toxicity to normal fibroblast cells (NIH-3T3) (Table 1). The compound **6j** emerged as a lead compound. The prolonged effect of compound **6j** was validated by clonogenic assay. The synthetic molecules with extended biological activities are considered as an effective drug [29,32]. Experimental evidence depicts that compound **6j** has significant long term cytotoxic effect against clonogenesis of A549, HepG2, A498, CaSki & SiHa cells (Fig. 2A–E).

2.2.2. Structure activity relationship (SAR)

A new series of the pyridazine derivatives have drawn much attention in the past decade due to their wide array of pharmacological activities [8,24]. Some of the pyridazine derivatives with altered substitutions have been reported to have a potential anti-proliferative efficiency [18]. In the search of anticancer drug, novel pyridazine analogues conjugated with multi structure having methyl, fluoro, chloro, bromo, nitro and isopropyl substitutions in the benzene ring were synthesized and assessed for its action against cancer proliferation. The experimental evidences highlighted that the compound with isopropyl group has potency to exhibit maximum sensitivity to cancer cells Table 1. The compound **6j** which has two isopropyl groups at ortho and para position as R and R₂ in the benzene moiety and the chloro group in the pyridazine ring at sixth position showed good activity at minimum inhibitory concentration (IC₅₀) of 6.6 ± 0.6, 6.9 ± 0.7, 6.8 ± 0.8, 7.5 ± 0.5 & 7.8 ± 0.4 μM against A549, HepG2, A498, CaSki & SiHa cells respectively. The other tested compounds with different substituent have shown moderate to minimal activity compared to **6j**. The compound **6f** with one isopropyl at ortho position of benzene ring showed the moderate cytotoxicity and compounds without isopropyl group depicted the minimal cytotoxic potency compared to compound **6j** which highlights the fundamental role of isopropyl group in



Scheme 1. Synthesis of novel pyridazine analogues 6a-l.

pyridazine's anti-cancer actions. Thus, it is evident that the presence of chloro and the isopropyl group with also their position of attachment in the pyridazine ring and benzene ring respectively as of compound **6j** is vital for the anti-neoplastic activity, as no other substitutions in the remaining compounds have exhibited significant cytotoxicity.

2.2.3. Compound **6j** counteracts the cancer cell migration and invasion

Most of the cancers, including lung, liver, renal, cervical and breast cancer etc., are extremely metastatic with increased migration and invasive characteristics [10,33–37]. To understand the role of compound **6j** in migration, we performed scratch wound assay with lung adenocarcinoma (A549) cells which is highly *in vitro* migratory. Migration of

Table 1

IC₅₀ values of Pyridazine analogs against various invasive cancer cell lines.

Compounds	Cytotoxicity(IC ₅₀) against cancer cells (μM)					
	A549	HepG2	A498	CaSki	SiHa	NIH-3T3
6a	94.3 ± 1.8	92.2 ± 2.2	90.5 ± 2.1	93.6 ± 1.3	89.8 ± 1.6	87.8 ± 1.8
6b	87.3 ± 1.3	84.2 ± 1.4	87.8 ± 0.5	82.6 ± 1.6	92.6 ± 1.3	84.2 ± 1.6
6c	38.7 ± 0.9	37.3 ± 0.8	41.6 ± 0.8	40.7 ± 1.2	39.1 ± 1.8	79.8 ± 1.3
6d	43.1 ± 0.7 [*]	45.4 ± 0.9	42.6 ± 1.3	44.6 ± 1.3	46.7 ± 1.4	99.1 ± 1.0
6e	75.1 ± 1.7	70.4 ± 1.6	85.3 ± 1.5	82.6 ± 1.7	88.1 ± 1.1	74.5 ± 1.6
6f	25.6 ± 0.4 ^{**}	23.7 ± 0.5 ^{**}	24.6 ± 0.7 [*]	26.7 ± 0.7 [*]	23.6 ± 0.8 [*]	89.8 ± 1.9
6g	96.8 ± 1.6	> 100	> 100	94.6 ± 1.8	> 100	99.6 ± 1.0
6h	46.8 ± 0.9	49.9 ± 1.1	48.6 ± 0.9	50.6 ± 1.3	49.6 ± 1.1	59.8 ± 1.6
6i	67.3 ± 0.6 [*]	63.1 ± 0.9	64.4 ± 1.7	72.6 ± 1.7	68.6 ± 1.3	64.5 ± 1.5
6j	6.6 ± 0.6 [*]	6.9 ± 0.7 [*]	6.8 ± 0.8 [*]	7.5 ± 0.5 ^{**}	7.8 ± 0.4 ^{**}	98.8 ± 1.4
6k	87.7 ± 1.5	82.6 ± 0.9	78.7 ± 1.5	82.6 ± 1.3	84.2 ± 1.4	54.8 ± 1.9
6l	98.1 ± 1.2	> 100	94.8 ± 0.9	> 100	> 100	99.8 ± 1.6
5-FU	7.4 ± 0.5 ^{**}	8.3 ± 1.8	5.4 ± 0.7 [*]	7.3 ± 0.4 ^{**}	8.3 ± 0.7 [*]	87.8 ± 1.3

Cytotoxicity was measured by MTT, Trypan blue and LDH release assays against each cell lines and average IC₅₀ values indicated in plus or minus ± standard deviation (SD). 5-Fluorouracil (5-FU) is used as a positive control. DMSO is used as a vehicle control which showed very negligible cytotoxicity. Statistically significant values are expressed as *p < 0.05 and **p < 0.01.

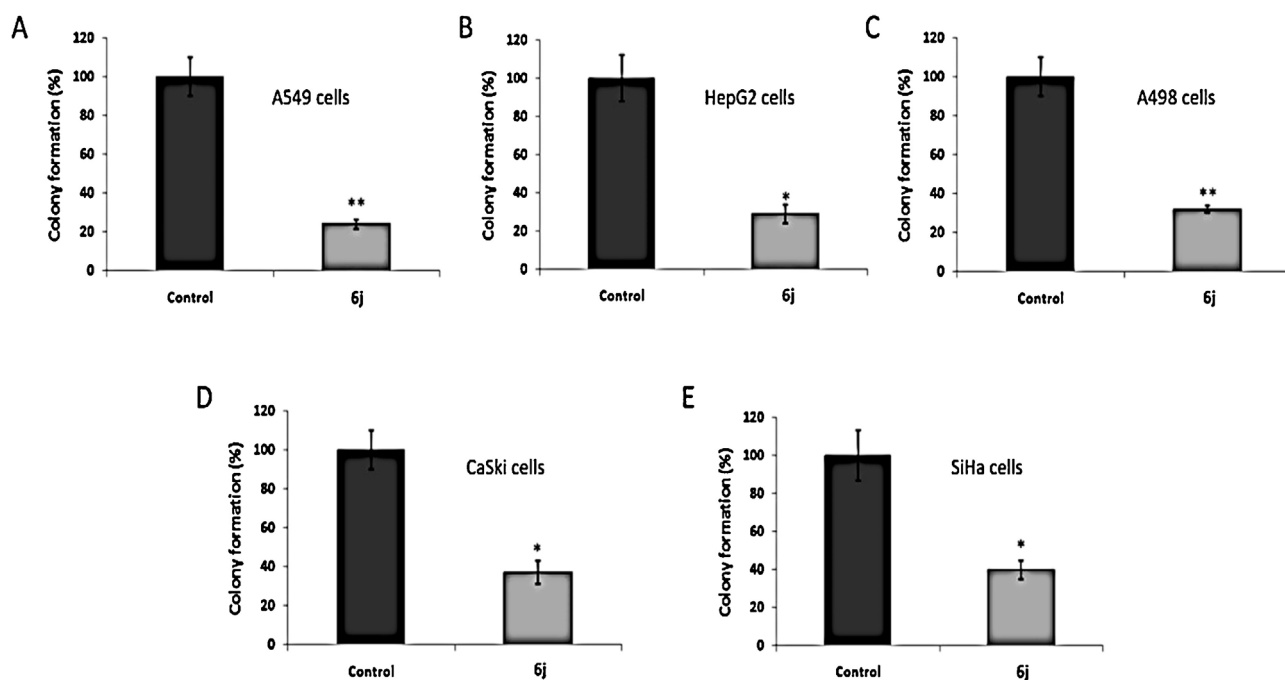


Fig. 2. Compound 6j exhibits a long term cytotoxic effect on conogenesis. The cells were cultured and exposed with and without compound 6j for 6 h and incubated for 12 days to form colonies; Compound 6j inhibits the clonogenic efficacy of (A) A549, (B) HepG2, (C) A498, (D) CaSki and (E) SiHa cells. Statistically significant values are expressed * $p < 0.05$ & ** $p < 0.01$.

cells into the wound was measured by capturing cell migration at 0 and 48 h post scratch. The A549 cells migrated over a period of 48 h to fill the wound, however, compound 6j treated cells failed to migrate into the wound and depicted a 78.21% of the decrease (Fig. 3A & B). The capability of neoplastic cells to invade is one of the major hallmarks of the metastatic process. To assess new anti-neoplastic agents for inhibiting this important process, the matrigel transwell invasion assay is an appropriate model that mimics the *in vivo* process [38]. The exposure of compound 6j reticence invasive potentials of A549 cancer cells on ECM gel with 86.6% inhibition whereas unexposed showed 100% invasion (Fig. 3C & D). Therefore, compound 6j has the potency to counteract the metastasis by targeting cancer cell migration and invasions.

2.2.4. Compound 6j abridges the expression of MMP-2 and MMP-9

During metastasis neoplastic, cell secretes matrix metalloproteinases including MMP-2 & -9 which are specifically capable of degrading ECM portions. Moreover, abnormal production of MMP-2 and MMP-9 facilitate cytoskeletal rearrangement, migration and invasion of cancer cells [38–41]. The compound 6j mediated MMPs alteration was investigated by immunoblots and gelatin zymography. Treatment of compound 6j inhibits the expression of MMP-2 and MMP-9 in invasive A549 cancer cells, which were apparent from immunoblot assessment (Fig. 3E). Furthermore, validation in gelatin zymography revealed that compound 6j reduces the gelatinase activity of MMP-2 and MMP-9 which reflects the potentiality of compound 6j on MMP inhibition (Fig. 3F), a synchronizing result of migration and invasion assays (Fig. 3A–D). It is clear that compound 6j inhibits the cancer cell migration and invasions by downregulating MMP-2 and MMP-9 expressions.

2.2.5. Compound 6j reticence the solid tumor development targeting MVD and MMPs expressions *in-vivo*

The physiological effect of compound 6j was assessed in the solid tumor (DLS) model. The solid tumour model is the most appropriate for preliminary screening and investigating pathophysiological potency of newly designed drugs [32]. The treatment of compound 6j on DL solid

tumor evidently impaired the tumor volume as measured by vernier caliper (Fig. 4A) and gradually repressed the tumor growth in dose dependent manner (Fig. 4B). The administration of compound 6j decreased the tumor development which is evident from physical morphology of mice bearing DLS (Fig. 4C). Physical appearance of thigh containing tumor demonstrates that compound 6j decreased DLS size evidently with 1.78 fold gram of tumor when compared to that of untreated (Fig. 4D). Toxicologically, compound 6j did not alter alkaline phosphatase (ALP), creatinine, urea, RBC and WBC level in serum (data not shown). H & E stain of DLS tumor postulated that compound 6j made a noteworthy reduction in microvascular density (MVD) with 12 ± 1.2 MVD/HPF compared to 33 ± 3.1 MVD/HPF of untreated (Fig. 4E). MMP-2 and MMP-9 immunostain of DLS reveal that compound 6j decreased the intra tumoural expression of MMP-2 and MMP-9, the critical tumourigenic factors in tumour angiogenesis and metastasis (Fig. 4F & G). As a consequence, survivability of DLS animals was prolonged up to 76th day when most of the untreated animals died before 35th day of tumor development (Fig. 4H).

2.2.6. Compound 6j interacts strongly with MMP-2 and MMP-9 protein *in-silico*

Following the promising potency of compound 6j on MMP inhibition under *in-vitro* and *in-vivo* conditions, the effect of compound 6j on MMP-2 and MMP-9 was validated by *in-silico* approach for elucidating the possible interaction of compound 6j with MMP-2 and MMP-9. Data revealed that compound 6j formed H-bond with ALA86, and an ionic interaction between carboxylic group of ALA86 and 'N' atom from pyridazine ring of the compound 6j which contributes to the most stable binding of the S1 conformation from ligand to MMP-2 with lowest Binding Energy at -8.16 kJ mol⁻¹ (Fig. 5A–D). Algorithmic study on compound 6j and MMP-9 demonstrated that compound 6j strongly interacted with LEU418 and TYR423 by H-bond which contributes to the most stable binding of the S9 conformation from ligand to MMP-9 with lowest Binding Energy at -9.81 kJ mol⁻¹ (Fig. 6A–D). Together, this *in-silico* results confirms the compound 6j action against the MMP-2 and MMP-9 mediated neoplastic growth.

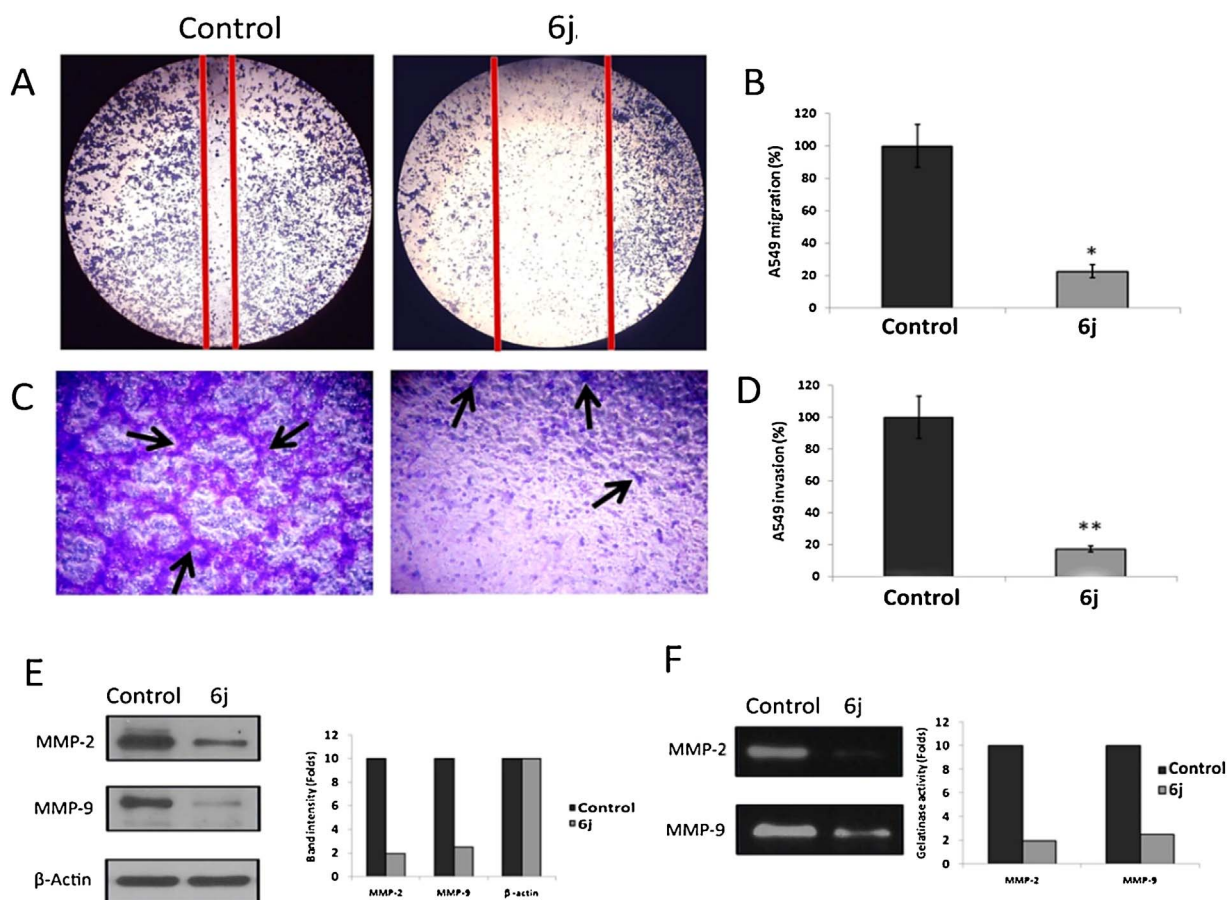


Fig. 3. Compound 6j impairs the cancer cell migration and invasions through down regulation of MMP-2 and MMP-9. The A549 monolayers were scratched to form wound and treated with compound 6j for 48 h; (A) Inhibition of A549 cell migration and (B) Graphical representation of cancer cell migration. The A549 cells were cultured on top of ECM gel coated invasion chamber, treated with compound 6j and complete media was added at the bottom of well and then incubated for 48 h; (C) Retention of A549 cell invasion in ECM gel and (D) Pictographical representation of A549 invasion. The A549 cells were cultured, treated with compound 6j and whole cell lysates and conditioned media was prepared. Immunoblots and gelatin zymography was performed; (E) Compound 6j inhibits MMP-2 and MMP-9 expression as verified by immunoblots and (F) Compound 6j counteracts the gelatinase activity of MMP-2 and MMP-9 as confirmed by zymography. Statistically significant values are expressed as * $p < 0.05$ & ** $p < 0.01$.

3. Conclusion

In summary, a novel series of pyridazine analogues **6a-l** were synthesized by incorporating, CH₃, F, Cl, Br, H, NO₂ and isopropyl groups and evaluated against metastatic neoplastic cells. Experimental evidences postulated that compound **6j** shows sensitivity to A549, HepG2, A498, CaSki and SiHa cells with extended cytotoxic effect. In addition, compound **6j** arrests the A549 migration and invasions markedly by counteracting MMP-2 and MMP-9 expressions. Also, compound **6j** proved its potentiality against DL solid tumor progression by abridging MVD and MMP expressions, a synchronizing result to *in-vitro* study. Compound **6j** interacted with MMP-2 and MMP-9 with H-bond *in-silico*, thereby down regulates the MMPs action in tumourigenesis. Altogether, we concluded that compound **6j** impairs cancer development and invasions through down regulation of MMP-2 and MMP-9 (Fig. 7).

4. Materials and methods

4.1. Experimental section

The chemicals required for the synthesis of title compounds **6a-l** were procured from Sigma Aldrich Chemical Co. The purity of the compounds was checked by thin layer chromatography (TLC) which was performed on aluminium-backed silica plates and the spots were detected by exposure to UV-lamp at $\lambda = 254$ nm. Melting points and boiling point were measured on a Chemiline, Microcontroller Based Melting Point/Boiling Point-CI725 Apparatus with a digital

thermometer. IR spectra were recorded on the Agilent Technologies Cary 630 FTIR spectrometer, ¹H and ¹³C NMR spectra were recorded on VNMRs-400 Agilent-NMR spectrophotometer. The mass spectra were obtained with a VG70-70H spectrometer and the elemental analysis (C, H, and N) was performed on Elementar Vario EL III elemental analyzer. The results of elemental analyses are within $\pm 0.4\%$ of the theoretical values.

4.2. Chemistry

4.2.1. General synthetic procedure for phenoxyacetic ethyl ester derivatives (**3a-l**)

A reaction of substituted phenols (**1a-l**, 0.025 mol) with chloroethyl acetate (**2**, 0.032 mol) in the presence of anhydrous potassium carbonate (0.075 mol) was refluxed in dry acetone (50 ml) for 10 h to afford phenoxyacetic ethyl esters (**3a-l**). The reaction was monitored by TLC using chloroform: hexane (3:1). The reaction mixture was cooled and the solvent was removed by distillation. The residual mass was poured into cold water to remove potassium carbonate and extracted with ether (3 \times 30 ml). The ether layer was washed with 10% sodium hydroxide solution, followed by water, then passed over anhydrous sodium sulfate to remove moisture and evaporated to afford liquid or pasty compounds **3a-l**.

4.2.1.1. Ethyl 2-phenoxyacetate (3a). Yield 80%; B.P. 98–101 °C; FT-IR (KBr, $\nu_{\text{maxcm}^{-1}}$): 1735–1759 (ester, C=O), 1150–1250 (ester, C–O); ¹H NMR (400 MHz, DMSO) δ (ppm): 1.32 (t, $J = 7$ Hz, 3H, CH₃ of

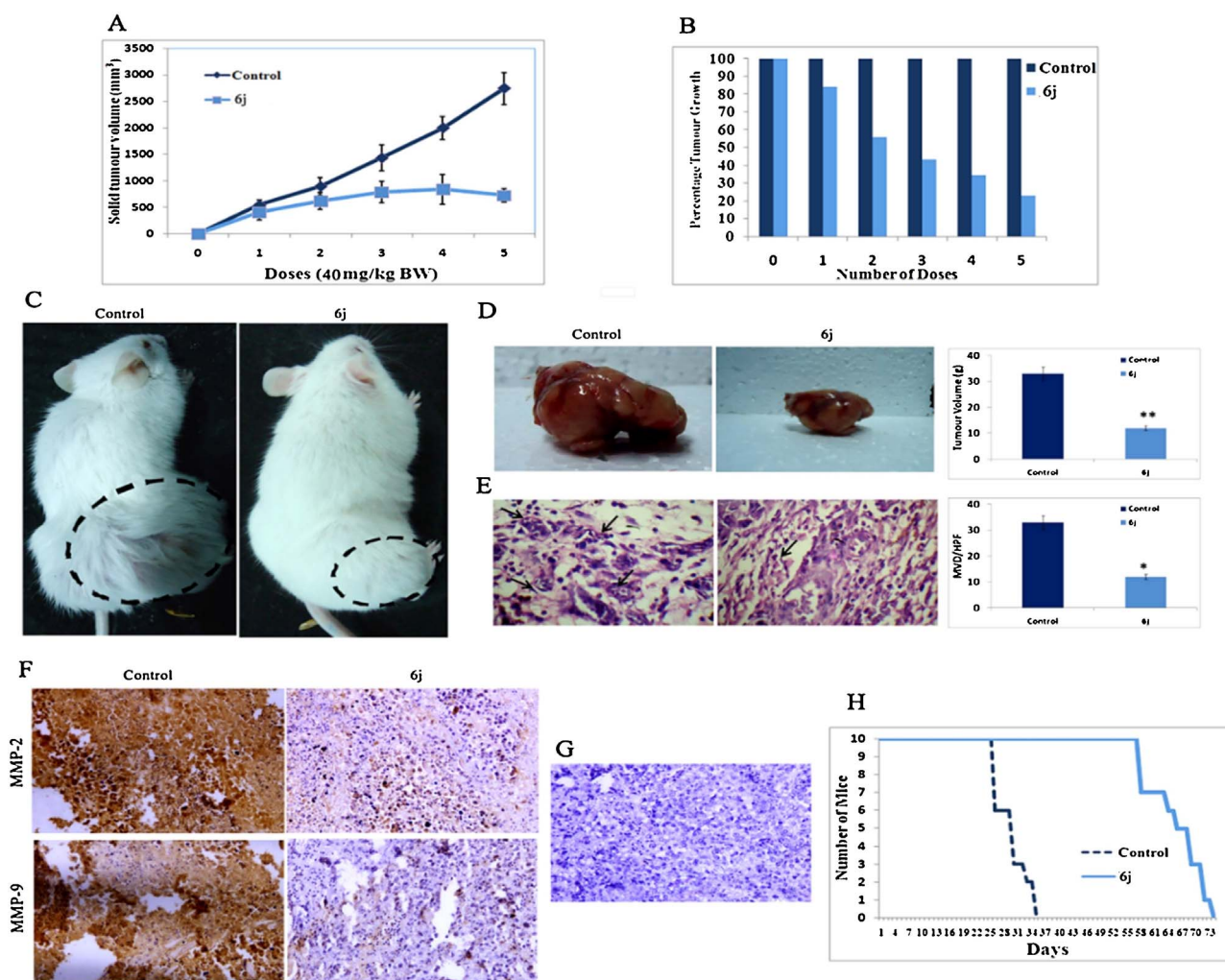


Fig. 4. Compound 6j reticence the DLS tumour development by counteracting MVD and MMP-2 & -9 expressions. DLS tumour was developed by culturing DLA cells in thigh region of mice subcutaneously and administered with compound 6j for 5 doses (ip) on every alternate days. On 35th day, tumor parameters, microvascular density and intra-tumoural MMP expressions were analysed. (A) Inhibition of DL solid tumour volume as measured by vernier caliper, (B) Graphical representation of dose dependant tumour inhibition, (C) Physical morphology of mice bearing DLS after compound 6j treatment, (D) Compound 6j exhibited decrease of tumour size and graphical representation of tumour mass, (E) Compound 6j lessened the DLS induced MVD and pictographical representation of MVD, (F) Compound 6j reduced intra-tumoural MMP-2 and MMP-9 expression as verified by immunohistochemistry, (G) Counter stain (immunohistochemistry) and (H) Compound 6j exhibited extended survivability. Statistically significant values are expressed as * $p < 0.05$ and ** $p < 0.0$.

ester), 4.24 (q, $J = 6$ Hz, 2H, CH₂ of ester), 5.01 (s, 2H, OCH₂), 6.77–7.34 (m, 5H, Ar-H); LC-MS m/z 181 [M+1]. Anal. Calcd for C₁₀H₁₂O₃ (180): C, 66.65; H, 6.71. Found: C, 66.59; H, 6.68%.

4.2.1.2. Ethyl 2-(2-bromophenoxy)acetate (3b). Yield 91%; B.P. 279–300 °C; FT-IR (KBr, ν_{\max} cm⁻¹): 1737–1755 (ester, C=O), 1155–1253 (ester, C–O); ¹H NMR (400 MHz, DMSO) δ (ppm): 1.20 (t, $J = 7$ Hz, 3H, CH₃ of ester), 4.16 (q, $J = 6$ Hz, 2H, CH₂ of ester), 4.76 (s, 2H, OCH₂), 6.86 (s, 1H, Ar-H₆), 6.92 (s, 1H, Ar-H₄), 7.33 (s, 1H, Ar-H₅), 7.63 (s, 1H, Ar-H₃); LC-MS m/z 259 [M+] and 261 [M+2]. Anal. Calcd. for C₁₀H₁₁BrO₃ (259): C, 46.36; H, 4.28. Found: C, 46.25; H, 4.19%.

4.2.1.3. Ethyl 2-(4-chloro-3-methylphenoxy)acetate (3c). Yield 73%; B.P. 114–116 °C; FT-IR (KBr, ν_{\max} cm⁻¹): 1737–1745 (ester, C=O), 1120–1260 (ester, C–O); ¹H NMR (400 MHz, DMSO) δ (ppm): 1.29 (t, $J = 7$ Hz, 3H, CH₃ of ester), 2.38 (s, 3H, CH₃), 4.34 (q, $J = 6$ Hz, 2H, CH₂ of ester), 5.55 (s, 2H, OCH₂), 6.77–7.34 (m, 3H, Ar-H); LC-MS m/z 229 [M+] and 231 [M+2]. Anal. Calcd for C₁₁H₁₃ClO₃ (229): C, 57.78; H, 5.73. Found: C, 57.63; H, 5.65%.

4.2.1.4. Ethyl 2-(o-tolylloxy)acetate (3d). Yield 88%; B.P. 259–261 °C;

FT-IR (KBr, ν_{\max} cm⁻¹): 1730–1740 (ester, C=O), 1115–1245 (ester, C–O); ¹H NMR (400 MHz, DMSO) δ (ppm): 1.43 (m, 3H, CH₃), 2.41 (s, 3H, CH₃), 4.24 (q, $J = 6$ Hz, 2H, CH₂ of ester), 5.08 (s, 2H, OCH₂), 6.97–7.34 (m, 4H, Ar-H); LC-MS m/z 195 [M+1]. Anal. Calcd for C₁₁H₁₄O₃ (194): C, 68.02; H, 7.27. Found: C, 68.01; H, 7.24%.

4.2.1.5. Ethyl 2-(2,4-difluorophenoxy)acetate (3e). Yield 75%; B.P. 263–266 °C; FT-IR (KBr, ν_{\max} cm⁻¹): 1728–1738 (ester, C=O), 1119–1258 (ester, C–O); ¹H NMR (400 MHz, DMSO) δ (ppm): 1.44 (t, $J = 7$ Hz, 3H, CH₃ of ester), 4.44 (q, $J = 6$ Hz, 2H, CH₂ of ester), 5.12 (s, 2H, OCH₂), 6.77–7.44 (m, 3H, Ar-H); LC-MS m/z 216 [M+]. Anal. Calcd for C₁₀H₁₀F₂O₃ (216): C, 55.56; H, 4.66. Found: C, 55.49; H, 4.58%.

4.2.1.6. Ethyl 2-(2-isopropylphenoxy)acetate (3f). Yield 85%; B.P. 300–303 °C; FT-IR (KBr, ν_{\max} cm⁻¹): 1738–1746 (ester, C=O), 1123–1266 (ester, C–O); ¹H NMR (400 MHz, DMSO) δ (ppm): 1.17 (d, $J = 8$ Hz, 6H, 2CH₃), 1.36 (t, $J = 7$ Hz, 3H, CH₃ of ester), 3.18 (m, H, CH), 4.74 (q, $J = 6$ Hz, 2H, CH₂ of ester), 5.91 (s, 2H, OCH₂), 6.17–7.24 (m, 4H, Ar-H); LC-MS m/z 223 [M+1]. Anal. Calcd for C₁₃H₁₈O₃ (222): C, 70.24; H, 8.16. Found: C, 70.19; H, 8.09%.

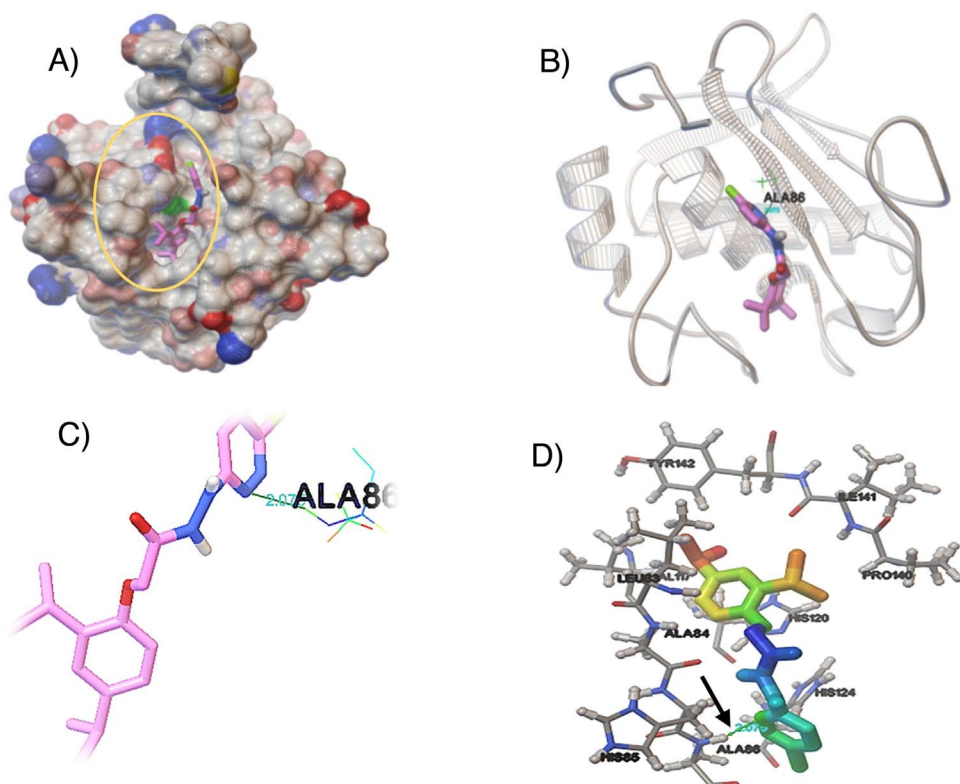


Fig. 5. Compound 6j interacts with MMP-2 for cancer regression *in-silico*. (A) Enfolding of molecules 6j in the active site pocket of MMP-2 complexes. (B) Ribbon models of MMP-2 catalytic domain and ligand molecules 6j complexes. (C) H-bond interaction of ligand molecule 6j with MMP-2. (D) The 2D interaction analysis of N'-(6-chloropyridazin-3-yl)-2-phenoxyacetohydrazide 6j with MMP-2.

4.2.1.7. Ethyl 2-(4-fluorophenoxy)acetate (3g). Yield 71%; B.P. 145–148 °C; FT-IR (KBr, $\nu_{\text{max}}\text{cm}^{-1}$): 1729–1743 (ester, C=O), 1126–1259 (ester, C–O); $^1\text{H NMR}$ (400 MHz, DMSO) δ (ppm): 1.29

(t, $J = 7$ Hz, 3H, CH_3 of ester), 4.64 (q, $J = 6$ Hz, 2H, CH_2 of ester), 5.11 (s, 2H, OCH_2), 7.09 (d, $J = 8.80$ Hz, 2H, Ar-H), 7.21 (d, $J = 8.80$ Hz, 2H, Ar-H); LC-MS m/z 198 $[\text{M}^+]$. Anal. Calcd for

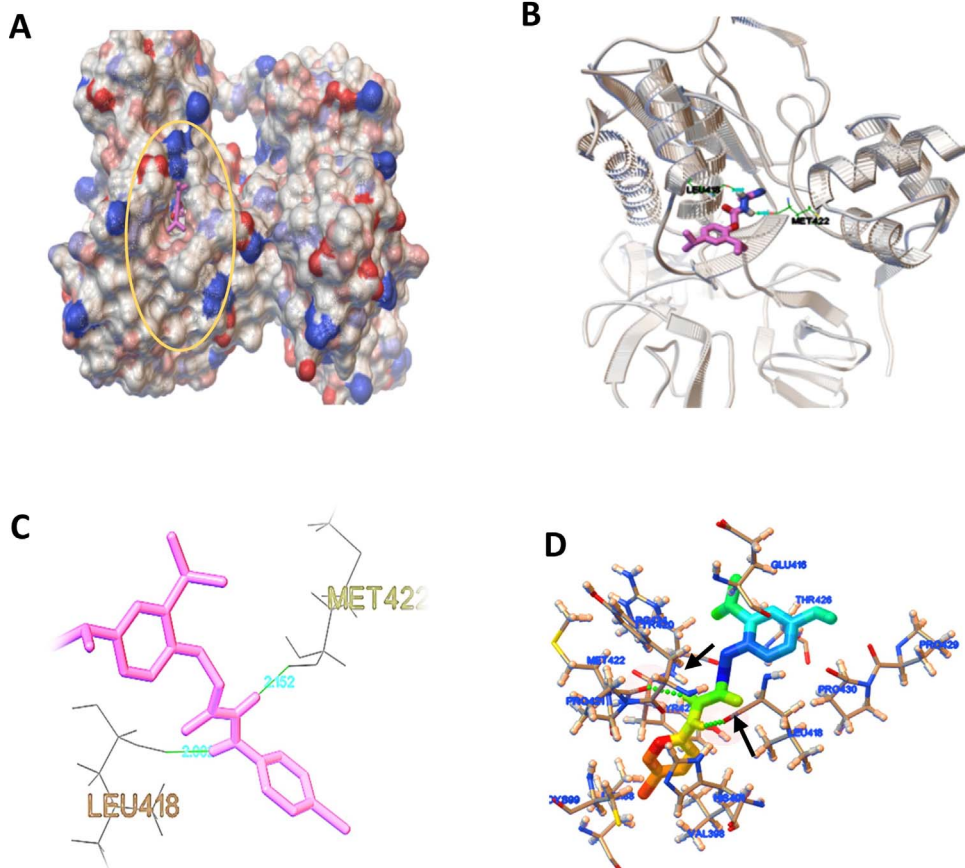


Fig. 6. Compound 6j interacts with MMP-9 for cancer regression *in-silico*. (A) Enfolding of molecules 6j in the active site pocket of MMP-9 complexes. (B) Ribbon models of MMP-9 catalytic domain and ligand molecules 6j complexes. (C) H-bond interaction of ligand molecule (6j) with MMP-9. (D) The 2D interaction analysis of N'-(6-chloropyridazin-3-yl)-2-phenoxyacetohydrazide 6j with MMP-9.

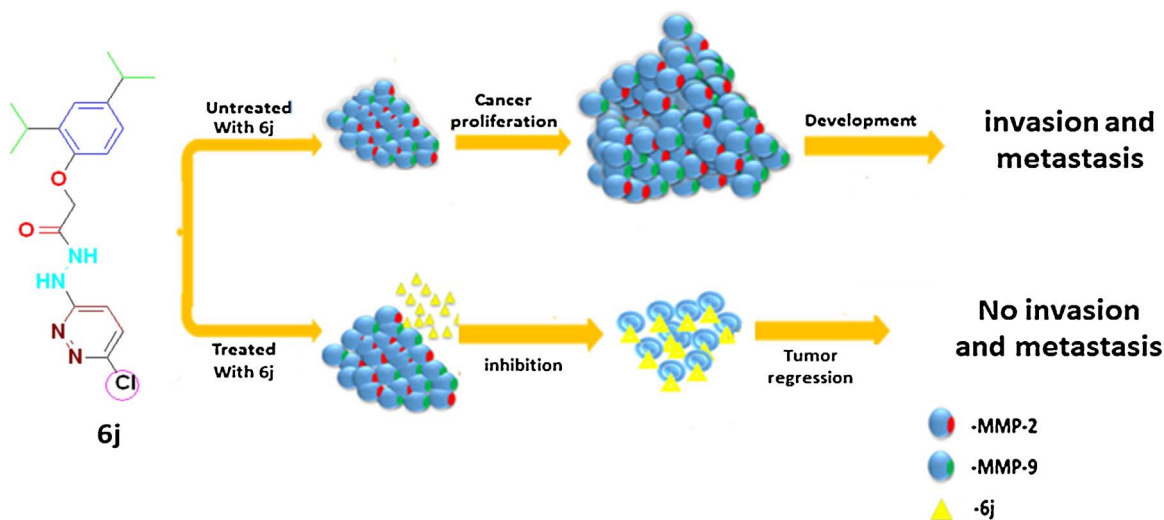


Fig. 7. Schematic representation of *N*-(6-chloropyridazin-3-yl)-2-(2,4 diisopropylphenoxy) acetohydrazide (**6j**) induced invasion and metastasis.

$C_{10}H_{11}FO_3$ (198): C, 60.60; H, 5.59. Found: C, 60.58; H, 5.56%.

4.2.1.8. Ethyl 2-(*p*-tolylloxy)acetate (3h). Yield 88%; B.P. 141–144 °C; FT-IR (KBr, $\nu_{\max} \text{cm}^{-1}$): 1731–1760 (ester, C=O), 1127–1259 (ester, C–O); $^1\text{H NMR}$ (400 MHz, DMSO) δ (ppm): 1.46 (t, $J = 7$ Hz, 3H, CH_3 of ester), 2.38 (s, 3H, CH_3), 4.55 (q, $J = 6$ Hz, 2H, CH_2 of ester), 5.04 (s, 2H, OCH_2), 6.94 (d, $J = 8.80$ Hz, 2H, Ar-H), 7.09 (d, $J = 8.80$ Hz, 2H, Ar-H); LC-MS m/z 195 [M+1]. Anal. Calcd for $C_{11}H_{14}O_3$ (194): C, 68.02; H, 7.27. Found: C, 68.01; H, 7.18%.

4.2.1.9. Ethyl 2-(4-chloro-2-fluorophenoxy)acetate (3i). Yield 77%; B.P. 285–288 °C; FT-IR (KBr, $\nu_{\max} \text{cm}^{-1}$): 1733–1744 (ester, C=O), 1126–1266 (ester, C–O); $^1\text{H NMR}$ (400 MHz, DMSO) δ (ppm): 1.29 (t, $J = 7$ Hz, 3H, CH_3 of ester), 4.34 (q, $J = 6$ Hz, 2H, CH_2 of ester), 5.31 (s, 2H, OCH_2), 6.27–7.84 (m, 3H, Ar-H); LC-MS m/z 233 [M+] and 235 [M+2]. Anal. Calcd for $C_{10}H_{10}ClFO_3$ (233): C, 51.63; H, 4.33. Found: C, 51.57; H, 4.29%.

4.2.1.10. Ethyl 2-(2,4-diisopropylphenoxy)acetate (3j). Yield 75%; Pasty mass; FT-IR (KBr, $\nu_{\max} \text{cm}^{-1}$): 1735–1750 (ester, C=O), 1120–1270 (ester, C–O); $^1\text{H NMR}$ (400 MHz, DMSO) δ (ppm): 1.20 (d, $J = 8$ Hz, 12H, 4 CH_3), 1.29 (t, $J = 7$ Hz, 3H, CH_3 of ester), 3.08 (m, 2H, 2CH), 3.59, 4.84 (q, $J = 6$ Hz, 2H, CH_2 of ester), 5.23 (s, 2H, OCH_2), 6.87–7.84 (m, 3H, Ar-H); LC-MS m/z 265 [M+1]. Anal. Calcd for $C_{16}H_{24}O_3$ (264): C, 72.69; H, 9.15. Found: C, 72.66; H, 9.13%.

4.2.1.11. Ethyl 2-(4-chlorophenoxy)acetate (3k). Yield 70%; B.P. 178–181 °C; FT-IR (KBr, $\nu_{\max} \text{cm}^{-1}$): 1733–1751 (ester, C=O), 1131–1256 (ester, C–O); $^1\text{H NMR}$ (400 MHz, DMSO) δ (ppm): 1.53 (t, $J = 7$ Hz, 3H, CH_3 of ester), 4.54 (q, $J = 6$ Hz, 2H, CH_2 of ester), 4.89 (s, 2H, OCH_2), 7.06 (d, $J = 8.80$ Hz, 2H, Ar-H), 7.35 (d, $J = 8.80$ Hz, 2H, Ar-H); LC-MS m/z 215 [M+] and 217 [M+2]. Anal. Calcd for $C_{10}H_{11}ClO_3$ (215): C, 55.96; H, 5.17. Found: C, 55.86; H, 5.09%.

4.2.1.12. Ethyl 2-(2-fluoro-4-nitrophenoxy)acetate (3l). Yield 65%; B.P. 358–360 °C; FT-IR (KBr, $\nu_{\max} \text{cm}^{-1}$): 1735–1755 (ester, C=O), 1126–1246 (ester, C–O); $^1\text{H NMR}$ (400 MHz, DMSO) δ (ppm): 1.37 (t, $J = 7$ Hz, 3H, CH_3 of ester), 5.24 (q, $J = 6$ Hz, 2H, CH_2 of ester), 5.77 (s, 2H, OCH_2), 7.34–8.34 (m, 3H, Ar-H); LC-MS m/z 243 [M+]. Anal. Calcd for $C_{10}H_{10}FNO_5$ (243): C, 49.39; H, 4.14; N, 5.76. Found: C, 49.27; H, 4.12; N, 5.64%.

4.2.2. General synthetic procedure for phenoxyacetic acid analogues (4a-I)

Phenoxy acetic acid ethyl esters (**3a-I**, 0.02 mol) were dissolved in ethanol (15 ml), 40% sodium hydroxide solution (2 ml) was added and the mixture was refluxed for 5–9 h. The reaction was monitored by TLC using hexane: ethyl acetate: methanol (5:2:1). The reaction mixture was cooled and quenched with 2 N hydrochloric acid. The precipitate was filtered, washed with water and finally recrystallized to afford compounds **4a-I**.

4.2.2.1. 2-Phenoxyacetic acid (4a). Yield 81%; M.P. 98–100 °C; FT-IR (KBr, $\nu_{\max} \text{cm}^{-1}$): 1714–1725 (C=O), 1246–1253 (Ar–O–C), 3377–3388 (OH); $^1\text{H NMR}$ (400 MHz, DMSO) δ (ppm): 4.66 (s, 2H, OCH_2), 6.79–7.35 (m, 5H, Ar-H), 13.11 (bs, 1H, OH); LC-MS m/z 152 [M+]. Anal. Calcd. for $C_8H_8O_3$ (152): C, 63.15; H, 5.30. Found: C, 63.08; H, 5.27%.

4.2.2.2. 2-(2-Bromophenoxy) acetic acid (4b). Yield 91%; M.P. 217–220 °C; FT-IR (KBr, $\nu_{\max} \text{cm}^{-1}$): 1715–1730 (C=O), 1250–1255 (Ar–O–C), 3375–3399 (OH); $^1\text{H NMR}$ (400 MHz, DMSO) δ (ppm): 4.71 (s, 2H, OCH_2), 6.86 (s, 1H, Ar-H₆), 6.92 (s, 1H, Ar-H₄), 7.33 (s, 1H, Ar-H₅), 7.63 (s, 1H, Ar-H₆), 14.09 (bs, 1H, OH); LC-MS m/z 231 [M+], 233 [M+2]. Anal. Calcd. for $C_8H_7BrO_3$ (231): C, 41.59; H, 3.05. Found: C, 41.52; H, 3.01%.

4.2.2.3. 2-(4-Chloro-3-methylphenoxy) acetic acid (4c). Yield 77%; M.P. 115–117 °C; FT-IR (KBr, $\nu_{\max} \text{cm}^{-1}$): 1710–1720 (C=O), 1245–1253 (Ar–O–C), 3366–3396 (OH); $^1\text{H NMR}$ (400 MHz, DMSO) δ (ppm): 2.46 (s, 3H, CH_3), 4.56 (s, 2H, OCH_2), 6.61–7.54 (m, 3H, Ar-H), 13.14 (bs, 1H, OH); LC-MS m/z 201 [M+], 203 [M+2]. Anal. Calcd. for $C_9H_9ClO_3$ (201): C, 53.88; H, 4.52. Found: C, 53.78; H, 4.49%.

4.2.2.4. 2-(*o*-Tolylloxy)acetic acid (4d). Yield 86%; M.P. 152–155 °C; FT-IR (KBr, $\nu_{\max} \text{cm}^{-1}$): 1720–1740 (C=O), 1240–1250 (Ar–O–C), 3379–3422 (OH); $^1\text{H NMR}$ (400 MHz, DMSO) δ (ppm): 2.19 (s, 3H, CH_3), 4.69 (s, 2H, OCH_2), 7.01–7.65 (m, 4H, Ar-H), 12.99 (bs, 1H, OH); LC-MS m/z 167 [M+1]. Anal. Calcd. for $C_9H_{10}O_3$ (166): C, 65.05; H, 6.07. Found: C, 65.01; H, 6.01%.

4.2.2.5. 2-(2,4-Difluorophenoxy)acetic acid (4e). Yield 79%; M.P. 124–127 °C; FT-IR (KBr, $\nu_{\max} \text{cm}^{-1}$): 1724–1745 (C=O), 1253–1256 (Ar–O–C), 3375–3391 (OH); $^1\text{H NMR}$ (400 MHz, DMSO) δ (ppm): 4.77 (s, 2H, OCH_2), 6.92–7.38 (m, 3H, Ar-H), 13.20 (bs, 1H, OH); LC-MS m/z 188 [M+]. Anal. Calcd. for $C_8H_6F_2O_3$ (188): C, 51.08; H, 3.21. Found: C, 51.04; H, 3.18%.

4.2.2.6. 2-(2-Isopropylphenoxy) acetic acid (4f). Yield 69%; M.P. 132–135 °C; FT-IR (KBr, $\nu_{\text{maxcm}^{-1}}$): 1715–1735 (C=O), 1249–1258 (Ar–O–C), 3355–3473 (OH); $^1\text{H NMR}$ (400 MHz, DMSO) δ (ppm): 1.17 (d, $J = 8$ Hz, 6H, CH₃), 3.11 (m, H, CH), 4.89 (s, 2H, OCH₂), 6.92–8.01 (m, 4H, Ar-H), 14.02 (bs, 1H, OH); LC–MS m/z 195 [M+1]. Anal. Calcd. for C₁₁H₁₄O₃ (194): C, 68.02; H, 7.27. Found: C, 68.00H, 7.19%.

4.2.2.7. 2-(4-Fluorophenoxy)acetic acid (4g). Yield 73%; M.P. 103–106 °C; FT-IR (KBr, $\nu_{\text{maxcm}^{-1}}$): 1725–1755 (C=O), 1250–1260 (Ar–O–C), 3345–3380 (OH); $^1\text{H NMR}$ (400 MHz, DMSO) δ (ppm): 4.59 (s, 2H, OCH₂), 7.09 (d, $J = 8.80$ Hz, 2H, Ar-H), 7.02–7.09 (d, $J = 8.80$ Hz, 2H, Ar-H), 13.93 (bs, 1H, OH); LC–MS m/z 170 [M+]. Anal. Calcd. for C₈H₇FO₃ (170): C, 56.48; H, 4.15. Found: C, 56.39; H, 4.09%.

4.2.2.8. (4-Methylphenoxy)acetic acid (4h). Yield 81%; M.P. 142–144 °C; FT-IR (KBr, $\nu_{\text{maxcm}^{-1}}$): 1730–1745 (C=O), 1253–1262 (Ar–O–C), 3375–3380 (OH); $^1\text{H NMR}$ (400 MHz, DMSO) δ (ppm): 2.39 (s, 3H, CH₃), 4.66 (s, 2H, OCH₂), 6.79–6.84 (d, $J = 8.80$ Hz, 2H, Ar-H), 7.03–7.09 (d, $J = 8.80$ Hz, 2H, Ar-H), 13.13 (bs, 1H, OH); LC–MS m/z 167 [M+1]. Anal. Calcd. for C₉H₁₀O₃ (166): C, 65.05; H, 6.07. Found: C, 65.02; H, 6.04%.

4.2.2.9. 2-(4-Chloro-2-fluorophenoxy)acetic acid (4i). Yield 76%; M.P. 62–65 °C; FT-IR (KBr, $\nu_{\text{maxcm}^{-1}}$): 1735–1755 (C=O), 1247–1257 (Ar–O–C), 3354–3386 (OH); $^1\text{H NMR}$ (400 MHz, DMSO) δ (ppm): 4.78 (s, 2H, OCH₂), 6.83–8.85 (m, 3H, Ar-H), 12.98 (bs, 1H, OH); LC–MS m/z 205 [M+], 207 [M+2]. Anal. Calcd. for C₈H₆ClFO₃ (205): C, 46.97; H, 2.96. Found: C, 46.89; H, 2.87%.

4.2.2.10. 2-(2,4-Diisopropylphenoxy)acetic acid (4j). Yield 78%; M.P. 82–85 °C; FT-IR (KBr, $\nu_{\text{maxcm}^{-1}}$): 1725–1748 (C=O), 1258–1260 (Ar–O–C), 3348–3399 (OH); $^1\text{H NMR}$ (400 MHz, DMSO) δ (ppm): 1.21 (d, $J = 8$ Hz, 12H, 4CH₃), 3.09 (m, 2H, 2CH), 4.69 (s, 2H, OCH₂), 5.99–7.45 (m, 3H, Ar-H), 13.26 (bs, 1H, OH); LC–MS m/z 237 [M+1]. Anal. Calcd. for C₁₄H₂₀O₃ (236): C, 71.16; H, 8.53. Found: C, 71.06; H, 8.48%.

4.2.2.11. 4-Chlorophenoxyacetic acid (4k). Yield 88%; M.P. 155–158 °C; FT-IR (KBr, $\nu_{\text{maxcm}^{-1}}$): 1701–1725 (C=O), 1243–1253 (Ar–O–C), 3375–3376 (OH); $^1\text{H NMR}$ (400 MHz, DMSO) δ (ppm): 4.58 (s, 2H, OCH₂), 7.09 (d, $J = 8.80$ Hz, 2H, Ar-H), 7.38 (d, $J = 8.80$ Hz, 2H, Ar-H), 14.02 (bs, 1H, OH); LC–MS m/z 187 [M+], 189 [M+2]. Anal. Calcd. for C₈H₇ClO₃ (187): C, 51.50; H, 3.78. Found: C, 51.48; H, 3.69%.

4.2.2.12. 2-(2-Fluoro-4-nitrophenoxy) acetic acid (4l). Yield 87%; M.P. 139–141 °C; FT-IR (KBr, $\nu_{\text{maxcm}^{-1}}$): 1722–17265 (C=O), 1244–1254 (Ar–O–C), 3369–3380 (OH); $^1\text{H NMR}$ (400 MHz, DMSO) δ (ppm): 4.67 (s, 2H, OCH₂), 7.26–8.09 (m, 3H, Ar-H), 12.03 (bs, 1H, OH); LC–MS m/z 215 [M+]. Anal. Calcd. for C₈H₆FNO₅ (215): C, 44.66; H, 2.81; N, 6.51. Found: C, 44.57; H, 2.79; N, 6.47%.

4.2.3. General synthetic procedure for 3-chloro-6-hydrazinylpyridazine (5b)

After stirring the compound 3,6-dichloropyridazine (5a, 2 mmol) in ethanol (20 ml) for 15 min at room temperature, hydrazine hydrate (2 mmol) was added. Further, the reaction was refluxed for 1 h at 100 °C and it was monitored by TLC using hexane: ethyl acetate (2:1) as the mobile phase. The white product of 3-chloro-6-hydrazinylpyridazine (5b) was filtered, washed and after drying, recrystallized from ethanol. Yield 62%; M.P. 136–138 °C; FT-IR (KBr, $\nu_{\text{maxcm}^{-1}}$): 1178–1181 (C=N), 3327–3139 (hydrazine NHNH₂), $^1\text{H NMR}$ (400 MHz, DMSO) δ (ppm): 4.59 (bs, 2H, NH₂), 7.21 (d, $J = 8$ Hz, 2H, Ar-H), 8.48 (s, 1H, NH); LC–MS m/z 145 [M+], 147 [M+2]. Anal. Calcd. for C₄H₅ClN₄ (145): C, 33.23; H, 3.49; N, 38.76. Found: C, 33.21; H, 3.47; N, 38.73%.

4.2.4. General synthetic procedure for N'-(6-chloropyridazin-3-yl)-2-phenoxyacetohydrazide analogues (6a-l)

To phenoxyacetic acids (4a-l, 2 mmol) stirring in dry DCM (20 ml), lutidine (3 mmol) was added at 25–30 °C, followed by the addition of 3-chloro-6-hydrazinylpyridazine (5b, 2 mmol). The reaction mixture was stirred at the same temperature for 30 min. After reducing the temperature to 0–5 °C, TBTU (2 mmol) was added to the mixture. The temperature was maintained below 5 °C over a period of 30 min. The reaction mass was stirred overnight and monitored by TLC. The solvent was evaporated under reduced pressure, quenched by the addition of crushed ice and the obtained solid was filtered, dried. This crude product was subjected to column chromatography and eluted with the solvent mixture of ethyl acetate: hexane (8:2) to get the pure product and was recrystallized to afford compounds 6a-l in good yield.

4.2.4.1. N'-(6-Chloropyridazin-3-yl)-2-phenoxyacetohydrazide (6a). Yield 82%; M.P. 160–162 °C; FT-IR (KBr, $\nu_{\text{maxcm}^{-1}}$): 1674 (C=O), 3120–3220 (NH–NH); $^1\text{H NMR}$ (400 MHz, DMSO) δ (ppm): 4.76 (s, 2H, OCH₂), 7.92–7.75 (m, 7H, Ar-H), 10.10 (s, 1H, NH), 10.30 (s, 1H, NH); $^{13}\text{C NMR}$ (100 MHz, DMSO): δ 66.82, 115.16, 120.08, 121.25, 129.25, 130.55, 154.3, 159.50, 162.01, 167.74; LC–MS m/z 279 [M+], 281 [M+2]. Anal. Calcd. For C₁₂H₁₁ClN₄O₂ (279): C, 51.72; H, 3.98; N, 20.10. Found: C, 51.78; H, 3.94; N, 20.06%.

4.2.4.2. 2-(2-Bromophenoxy)-N'-(6-chloropyridazin-3-yl)acetohydrazide (6b). Yield 78%; M.P. 170–172 °C; FT-IR (KBr, $\nu_{\text{maxcm}^{-1}}$): 1644 (C=O), 3109–3121 (NH–NH); $^1\text{H NMR}$ (400 MHz, DMSO) δ (ppm): 4.79 (s, 2H, OCH₂), 6.83–8.09 (m, 6H, Ar-H), 8.90 (s, 1H, NH), 11.03 (s, 1H, NH); $^{13}\text{C NMR}$ (100 MHz, DMSO): δ 67.01, 111.12, 113.29, 120.09, 123.91, 129.18, 130.18, 133.99, 151.50, 154.9, 162.04, 166.74; LC–MS m/z 358 [M+], 360 [M+2], 362 [M+4]. Anal. Calcd. For C₁₂H₁₀BrClN₄O₂: C, 40.31; H, 2.82; N, 15.67. Found: C, 40.29; H, 2.80; N, 15.64%.

4.2.4.3. 2-(4-Chloro-3-methylphenoxy)-N'-(6-chloropyridazin-3-yl)acetohydrazide (6c). Yield 76%; M.P. 129–131 °C; FT-IR (KBr, $\nu_{\text{maxcm}^{-1}}$): 1663 (C=O), 3137–3250 (NH–NH); $^1\text{H NMR}$ (400 MHz, DMSO) δ (ppm): 2.35 (s, 3H, CH₃), 4.01 (s, 2H, OCH₂), 7.01–7.99 (m, 5H, Ar-H), 9.06 (s, 1H, NH), 10.98 (s, 1H, NH); $^{13}\text{C NMR}$ (100 MHz, DMSO): δ 21.28, 67.79, 114.08, 114.59, 119.99, 128.92, 129.55, 130.17, 133.81, 152.39, 158.59, 163.03, 166.95; LC–MS m/z 327 [M+], 329 [M+2], 331 [M+4]. Anal. Calcd. For C₁₃H₁₂Cl₂N₄O₂ (327): C, 47.73; H, 3.70; N, 17.13. Found: C, 47.73; H, 3.69; N, 17.11%.

4.2.4.4. N'-(6-Chloropyridazin-3-yl)-2-(o-tolylxy)acetohydrazide (6d). Yield 83%; M.P. 128–130 °C; FT-IR (KBr, $\nu_{\text{maxcm}^{-1}}$): 1649 (C=O), 3119–3259 (NH–NH); $^1\text{H NMR}$ (400 MHz, DMSO) δ (ppm): 2.15 (s, 3H, CH₃), 5.01 (s, 2H, OCH₂), 6.89–7.35 (m, 6H, Ar-H), 8.97 (s, 1H, NH), 10.49 (s, 1H, NH); $^{13}\text{C NMR}$ (100 MHz, DMSO): δ 16.02, 65.99, 113.22, 119.73, 121.29, 125.77, 126.90, 129.91, 132.06, 152.03, 159.25, 162.19, 167.43; LC–MS m/z 293 [M+], 295 [M+2]. Anal. Calcd. For C₁₃H₁₃ClN₄O₂ (293): C, 53.34; H, 4.48; N, 19.14. Found: C, 53.32; H, 4.44; N, 19.11%.

4.2.4.5. N'-(6-Chloropyridazin-3-yl)-2-(2,4-difluorophenoxy)acetohydrazide (6e). Yield 78%; M.P. 122–124 °C; FT-IR (KBr, $\nu_{\text{maxcm}^{-1}}$): 1657 (C=O), 3110–3222 (NH–NH); $^1\text{H NMR}$ (400 MHz, DMSO) δ (ppm): 4.55 (s, 2H, OCH₂), 7.44–8.11 (m, 5H, Ar-H), 9.05 (s, 1H, NH), 9.99 (s, 1H, NH); $^{13}\text{C NMR}$ (100 MHz, DMSO): δ 67.19, 107.17, 113.11, 118.04, 119.92, 129.82, 146.11, 152.33, 153.04, 154.11, 162.07, 167.08; LC–MS m/z 315 [M+], 317 [M+2]. Anal. Calcd. For C₁₂H₉ClF₂N₄O₂ (315): C, 45.80; H, 2.88; N, 17.80. Found: C, 45.78; H, 2.86; N, 17.76%.

4.2.4.6. N'-(6-Chloropyridazin-3-yl)-2-(2-isopropylphenoxy)acetohydrazide (6f). Yield 78%; M.P. 132–134 °C; FT-IR (KBr,

$\nu_{\max} \text{cm}^{-1}$): 1661 (C=O), 3107–3248 (NH–NH); ^1H NMR (400 MHz, DMSO) δ (ppm): 1.14 (d, $J = 7.40$ Hz, 6H, 2CH₃), 3.05 (m, 1H, CH), 5.55 (s, 2H, OCH₂), 6.91–7.52 (m, 6H, Ar-H), 8.93 (s, 1H, NH), 11.01 (s, 1H, NH); ^{13}C NMR (100 MHz, DMSO): δ 23.67, 27.64, 66.96, 113.19, 119.65, 120.76, 126.05, 127.17, 129.93, 136.54, 152.39, 156.53, 161.57, 164.98; LC–MS m/z 321 [M+] 323 [M+2]. Anal. Calcd. For C₁₅H₁₇ClN₄O₂ (321): C, 56.17; H, 5.34; N, 17.47. Found: C, 56.13; H, 5.31; N, 17.44%.

4.2.4.7. *N'*-(6-Chloropyridazin-3-yl)-2-(4-fluorophenoxy)acetohydrazide (6g). Yield 77%; M.P 104–106 °C; FT-IR (KBr, $\nu_{\max} \text{cm}^{-1}$): 1679 (C=O), 3129–3239 (NH–NH); ^1H NMR (400 MHz, DMSO) δ (ppm): 4.29 (s, 2H, OCH₂), 7.03–7.69 (m, 6H, Ar-H), 9.01 (s, 1H, NH), 10.90 (s, 1H, NH); ^{13}C NMR (100 MHz, DMSO): δ 69.16, 116.96, 117.45, 120.29, 129.21, 152.13, 154.95, 156.34, 163.03, 166.98; LC–MS m/z 297 [M+] 299 [M+2]. Anal. Calcd. For C₁₂H₁₀ClFN₄O₂ (297): C, 48.58; H, 3.40; N, 18.88. Found: C, 48.55; H, 3.38; N, 18.86%.

4.2.4.8. *N'*-(6-Chloropyridazin-3-yl)-2-(*p*-tolylxy)acetohydrazide (6h). Yield 84%; M.P 127–129 °C; FT-IR (KBr, $\nu_{\max} \text{cm}^{-1}$): 1675 (C=O), 3124–3230 (NH–NH); ^1H NMR (400 MHz, DMSO) δ (ppm): 2.25 (s, 3H, CH₃), 4.71 (s, 2H, OCH₂), 6.89 (d, $J = 9.2$ Hz, 2H, Ar-H), 7.05 (d, $J = 9.2$ Hz, 1H, 4-pyridazin-H), 7.10 (d, $J = 9.2$ Hz, 2H, Ar-H) 7.20 (d, $J = 9.2$ Hz, 1H, 5-pyridazin-H), 8.99 (s, 1H, NH), 10.94 (s, 1H, NH); ^{13}C NMR (100 MHz, DMSO): δ 22.91, 67.29, 115.29, 119.87, 129.39, 130.01, 132.17, 152.38, 158.55, 164.06, 168.76; LC–MS m/z 293 [M+] 295 [M+2]. Anal. Calcd. For C₁₃H₁₃ClN₄O₂ (293): C, 53.34; H, 4.48; N, 19.14. Found: C, 53.32; H, 4.45; N, 19.12%.

4.2.4.9. 2-(4-Chloro-2-fluorophenoxy)- *N'*-(6-chloropyridazin-3-yl)acetohydrazide (6i). Yield 87%; M.P 146–148 °C; FT-IR (KBr, $\nu_{\max} \text{cm}^{-1}$): 1667 (C=O), 3126–3229 (NH–NH); ^1H NMR (400 MHz, DMSO) δ (ppm): 4.90 (s, 2H, OCH₂), 6.47–7.34 (m, 6H, Ar-H), 8.96 (s, 1H, NH), 11.19 (s, 1H, NH); ^{13}C NMR (100 MHz, DMSO): δ 65.93, 117.71, 118.55, 119.81, 127.59, 128.89, 129.81, 147.63, 151.43, 152.99, 163.01, 166.38; LC–MS m/z 331 [M+] 333 [M+2] 335 [M+4]. Anal. Calcd. For C₁₂H₉Cl₂FN₄O₂ (331): C, 48.58; H, 3.40; N, 18.88. Found: C, 48.55; H, 3.38; N, 18.86%.

4.2.4.10. *N'*-(6-Chloropyridazin-3-yl)-2-(2,4-diisopropylphenoxy)acetohydrazide (6j). Yield 84%; M.P 108–110 °C; FT-IR (KBr, $\nu_{\max} \text{cm}^{-1}$): 1683 (C=O), 3131–3220 (NH–NH); ^1H NMR (400 MHz, DMSO) δ (ppm): 1.14 (d, $J = 8.80$ Hz, 6H, 2CH₃), 1.20 (d, $J = 8.80$ Hz, 6H, 2CH₃), 2.87 (m, 1H, CH), 3.05 (m, 1H, CH), 4.55 (s, 2H, OCH₂), 6.75–7.59 (m, 5H, Ar-H), 8.49 (s, 1H, NH), 10.49 (s, 1H, NH); ^{13}C NMR (100 MHz, DMSO): δ 23.06, 24.17, 28.72, 34.48, 67.26, 113.09, 120.19, 125.29, 127.38, 129.99, 138.69, 140.74, 151.93, 152.96, 163.07, 167.39; LC–MS m/z 363 [M+] 365 [M+2]. Anal. Calcd. For C₁₈H₂₃ClN₄O₂ (363): C, 59.58; H, 6.39; N, 15.44. Found: C, 59.56; H, 6.36; N, 15.42%.

4.2.4.11. 2-(4-Chlorophenoxy)- *N'*-(6-chloropyridazin-3-yl)acetohydrazide (6k). Yield 79%; M.P 152–154 °C; FT-IR (KBr, $\nu_{\max} \text{cm}^{-1}$): 1671 (C=O), 3123–3228 (NH–NH); ^1H NMR (400 MHz, DMSO) δ (ppm): 4.71 (s, 2H, OCH₂), 7.04 (d, $J = 9.2$ Hz, 2H, Ar-H), 7.06 (d, $J = 9.2$ Hz, 1H, 4-pyridazin-H), 7.19 (d, $J = 9.2$ Hz, 1H, 5-pyridazin-H) 7.38 (d, $J = 9.2$ Hz, 2H, Ar-H), 8.88 (s, 1H, NH), 10.88 (s, 1H, NH); ^{13}C NMR (100 MHz, DMSO): δ 65.99, 117.34, 120.02, 126.86, 130.11, 132.39, 152.37, 157.02, 163.09, 167.03; LC–MS m/z 313 [M+] 315 [M+2] 317 [M+4]. Anal. Calcd. For C₁₂H₁₀Cl₂N₄O₂ (315): C, 46.03; H, 3.22; N, 18.89. Found: C, 46.01; H, 3.20; N, 18.86%.

4.2.4.12. *N'*-(6-Chloropyridazin-3-yl)-2-(2-fluoro-4-nitrophenoxy)acetohydrazide (6l). Yield 84%; M.P 112–114 °C; FT-IR (KBr, $\nu_{\max} \text{cm}^{-1}$): 1681 (C=O), 3129–3229 (NH–NH); ^1H NMR (400 MHz, DMSO) δ (ppm): 4.55 (s, 2H, CH₂), 7.03–8.06 (m, 5H, Ar-H), 8.77 (s,

1H, NH), 10.76 (s, 1H, NH); ^{13}C NMR (100 MHz, DMSO): δ 65.77, 115.82, 118.98, 122.73, 125.25, 126.21, 130.91, 141.98, 151.43, 161.77, 162.09, 166.73; LC–MS m/z 342 [M+] 344 [M+2]. Anal. Calcd. For C₁₂H₉ClFN₄O₄ (342): C, 42.18; H, 2.66; N, 20.50. Found: C, 42.15; H, 2.62; N, 20.48%.

4.3. Biological study

The human lung adenocarcinoma (A549), hepatocellular carcinoma (HepG2), renal carcinoma (A498) and cervical carcinoma (CaSki and SiHa) and normal fibroblast (NIH-3T3) cells were used for determining the IC₅₀ value of newly synthesized series 6a-l by MTT, trypan blue, LDH leak and clonogenic assays. Anti-migration and invasive efficacies of the lead compound was evaluated in A549 cells by migration and invasion assays, gelatin zymography and immunoblots.

4.3.1. Cell culture and cytotoxic studies

The A549, HepG2, A498, CaSki and SiHa cells were grown in DMEM medium (Gibco-Invitrogen, USA), supplemented with 10% FBS (Invitrogen, USA), sodium carbonate (0.37%) and Antibiotic-antimycotic solution (100 µg/ml) (Sigma-Aldrich, USA) at 37 °C with 5% CO₂ in a humidified carbon dioxide (CO₂) incubator. After serum starvation, the cells were exposed with diverse concentration of compounds 6a-l (0, 5, 10, 25, 50 and 100 µM in DMSO) and reincubated at 37 °C for 45 h. DMSO and 5-Fluorouracil were used as a vehicle and positive control respectively. MTT assay, trypan blue dye exclusion assay and LDH release assay were performed and cytotoxicity of compounds 6a-l was determined [42,43].

4.3.2. Clonogenic assay

Anti-clonogenic and extended effect of compound 6j (0 & 8 µM) against A549, HepG2, A498, CaSki and SiHa cells was assessed by performing clonogenic assay [32]. In concise, the cells (~400/well) were cultured and exposed with compound 6j for 6 h, cultured further for 12 days. Colonies were fixed with methanol, stained with crystal violet and counted.

4.3.3. Migration assay

The efficacy of the compound 6j on A549 cell migration was validated by performing migration assay with minor modifications [32]. The A549 was cultured in DMEM medium to form monolayer and 2 mm size wounds were made by scratching with a microtip. The wounds were exposed with compound 6j (0 & 8 µM), incubated for 48 h, fixed with methanol and stained in crystal violet (0.4 g/L). Cell migrations were photographed at identical locations using Olympus Phase Contrast inverted microscope. The potency of compound 6j on A549 cell migration was calculated by comparing the final gap width to initial gap width.

4.3.4. Matrigeltranswell invasion assay

Matrigel (ECM gel) transwell invasion assay was performed to investigate the anti-invasive efficacy of compound 6j as mentioned earlier [44]. In concise, Serum free medium containing of A549 (5 × 10⁴/well) cells was cultured with and without 6j (8 µM) on top of invasion chamber coated with ECM gel. DMEM with 10% FBS was supplied in the lower chamber and incubated at 37 °C for 24 h. Then invasion chamber was carefully removed and uninvasion cells on top of the invasion chamber were removed by wet cotton swab and invaded cells were fixed with methanol, stained with crystal violet (0.4 g/L). The effect of compound 6j on A549 invasion was assessed by counting invaded cells at the bottom of the chamber in Olympus Phase Contrast inverted microscope and photographed.

4.3.5. Gelatin zymography

Gelatin zymography is the most appropriate assay system to quantify the secretion of MMP-2 and MMP-9. In brief, A549 cells were

cultured and treated with and without 8 μM of compound **6j** for 48 h. Secreted proteins from conditioned media were quantified in Biospectrophotometer (Eppendorf, Germany) and resolved in 8% SDS-PAGE gels containing 0.1% (w/v) gelatin. Zymogram was developed as reported earlier [45] and decrease of gelatin lysis zones was documented using Bio-rad Gel Documentation™ XR + Imaging System.

4.3.6. Immunoblots

The whole cell lysates were prepared from compound **6j** treated and untreated A549 cells using RIPA buffer (100 mM Tris pH 7.5, 140 mM NaCl, 0.1% SDS, 5 mM EDTA, 1% Triton X-100, 0.5% sodium deoxycholate, 0.5 mM PMSF and Protease inhibitor cocktail) [32,46]. Cell lysates concentration was determined by using Biospectrophotometer and 30 μg of lysates were resolved 12% SDS-PAGE and transferred to PVDF membrane. Immunoblot analysis was carried out for MMP-2 and MMP-9 (Santacruz Biotechnology, USA) and β -actin (BD Bioscience, USA).

4.3.7. Animals and ethics

Male swiss albino mice (27–30 g) were used throughout the study. All the experiments performed on animals were reviewed and approved by National College of Pharmacy Ethical Committee, Shivamogga, India as per CPCSEA guidelines (NCP/IAEC/CL/101/05/2012-13).

4.3.8. Determination of LD50 and evaluation of side effects of compound **6j** in normal animals

The acute toxicity studies of the compound **6j** was evaluated in non-tumor bearing Swiss albino mice by intraperitoneal administration of compound **6j** (0, 100, 300, 500, 1000 mg/kg body weight ($n = 5$) and LD₅₀ was determined as per the standard CPCSEA guidelines. Following LD₅₀ assessment, treatment dose of compound **6j** was fixed at 40 mg/kg *bw* and further the animals bearing Dalton's solid lymphoma administered for anti-cancer investigations.

4.3.9. Tumor model and treatment

DLA cells were cultured in peritoneum of mice and exponentially growing DLA cells were withdrawn, re-injected (5×10^6 cells/thigh) into thigh region of the mice subcutaneously (*s.c.*) to develop DL solid tumor (DLS) [32]. After onset of tumor development (100 mm³ size), mice were administered with or without compound **6j** ($n = 5$ each, 40 mg/kg body weight) for 5 doses intraperitoneally on every alternate days. At the end of the 35th day, the tumor mass were separated and photographed. Tumor tissues were processed for H & E staining and immunohistochemistry (IHC) analysis as described earlier [32].

For assessing toxicological parameters of compound **6j**, serum was collected for alkaline phosphatase (ALP), creatinine, urea, RBC and WBC quantification. Survivability of mice bearing DLS of compound **6j** treated and untreated ($n = 10$ each) was monitored separately.

4.4. In-silico studies

The interaction of compound **6j** with MMPs (MMP- 2 & -9) was validated by performing molecular algorithmic study since it inhibits the action of MMP-2 and MMP-9. The MMP-2 and MMP-9 receptor domains were obtained from PDB: 1HOV (model 3: A) and PDB: 1L6J respectively and used it for the current investigation. The results of molecular docking were analyzed using autodock 4.2. Using tools available in autodock programmer the proteins and ligands were downloaded and prepared in three-dimensional atomic coordinates for molecular docking. A lamarkian genetic algorithm method was applied in the program suite was employed to recognize suitable binding modes and conformation of the ligand molecules. Also using autodock tools (ADT) gasteiger charges were added and the rotatable bonds were set and all torsions were allowed to rotate. Polar hydrogen atoms were added and kollaman charges were assigned to the protein using autodock tools (ADT). To each atom type grid maps were assigned in the

protein and ligand. Desolation maps and additional electrostatic were also calculated. Using the Lamarckian Genetic algorithm (LGA), Molecular docking simulations were performed as the search algorithm. All molecular modeling experiments were carried out with carton and ribbon models and the figures showing protein-ligand interactions were generated using PyMOL [47,48].

4.5. Statistical analysis

Values were expressed as mean \pm standard deviation (SD). MS excel 8.1 version software was used for data analysis, statistical significance was evaluated by one-way analysis of variance (ANOVA) followed by 2-tailed Student's *t*-test. Statistical significant values were expressed as **p* < 0.05 and ***p* < 0.01.

Conflict of interest statement

The authors declare that there are no conflicts of interest.

Acknowledgements

Yasser Hussein Eissa Mohammed is thankful to the University of Hajjah, Yemen, for providing financial assistance under the teacher's fellowship. Zabiulla gratefully acknowledges the financial support provided by the Department of Science and Technology, New Delhi, Under INSPIRE-Fellowship scheme [IF140407]. Shaukath Ara Khanum expresses sincere gratitude to the Government of Karnataka, Vision Group on Science and Technology, Bangalore for the financial assistance and support [VGST/CISEE/2012-13/282 dated 16th March 2013] and UGC, New Delhi under the Major Research Project Scheme [F.39/737/2010 (SR)]. B.T. Prabhakar gratefully acknowledges the grant extended by DBT (6242-P37/RGCB/PMD/DBT/PBKR/2015), UGC F.No.41-507/2012 (SR) and VGST (VGST/GRD231/CISEE/2013-14).

Appendix A. Supplementary data

Supplementary data associated with this article can be found, in the online version, at <http://dx.doi.org/10.1016/j.biopha.2017.08.105>.

References

- [1] R.D. Loberg, D.A. Bradley, S.A. Tomlins, A.M. Chinnaiyan, K.J. Pienta, The lethal phenotype of cancer: the molecular basis of death due to malignancy, *CA. Cancer J. Clin.* 57 (2007) 225–241.
- [2] R. Siegel, E. Ward, O. Brawley, A. Jemal, Cancer statistics, 2011: the impact of eliminating socioeconomic and racial disparities on premature cancer deaths, *CA. Cancer J. Clin.* 61 (2011) 212–236.
- [3] N. Kramer, A. Walzl, C. Unger, M. Rosner, G. Krupitza, M. Hengstschlager, H. Dolznig, In vitro cell migration and invasion assays, *Mutat. Res. Rev. Mutat. Res.* 752 (2013) 10–24.
- [4] A.G. Clark, D.M. Vignjevic, Modes of cancer cell invasion and the role of the microenvironment, *Curr. Opin. Cell Biol.* 36 (2015) 13–22.
- [5] P.S. Steeg, Tumor metastasis: mechanistic insights and clinical challenges, *Nat. Med.* 12 (2006) 895–904.
- [6] K. Kessenbrock, V. Plaks, Z. Werb, Matrix metalloproteinases: regulators of the tumor microenvironment, *Cell* 141 (2010) 52–67.
- [7] P. Friedl, S. Alexander, Cancer invasion and the microenvironment: plasticity and reciprocity, *Cell* 147 (2011) 992–1009.
- [8] P. Friedl, Y. Hegerfeldt, M. Tusch, Collective cell migration in morphogenesis and cancer, *Int. J. Dev. Biol.* (2004) 441–449.
- [9] N.V. Krakhmal, M.V. Zavyalova, E.V. Denisov, S.V. Vtorushin, Perelmuter, cancer invasion: patterns and mechanisms, *Acta Naturae* 7 (2015) 17.
- [10] F.V. Zijl, G. Krupitza, W. Mikulits, Initial steps of metastasis: cell invasion and endothelial transmigration, *Mutat. Res.* 728 (2011) 23–34.
- [11] N. Adhikari, A. Mukherjee, A. Saha, T. Jha, Arylsulfonamides and selectivity of matrix Metalloproteinase-2: an overview, *Eur. J. Med. Chem.* 129 (2017) 72–109, <http://dx.doi.org/10.1016/j.ejmech.2017.02.014>.
- [12] S.A. Amin, N. Adhikari, T. Jha, Is dual inhibition of metalloenzymes HDAC-8 and MMP-2 a potential pharmacological target to combat hematological malignancies? *Pharmacol. Res.* 122 (2017) 8–19.
- [13] S.A. Khanum, S. Shashikanth, S. Umeha, R. Kavitha, Synthesis and antimicrobial study of novel heterocyclic compounds from hydroxybenzophenones, *Eur. J. Med. Chem.* 40 (2005) 1162.

- [14] N.O. Al-Harbi, S.A. Bahashwan, K.A. Shadid, Anti-inflammatory, analgesic and antiparkinsonism activities of some novel pyridazine derivatives, *J. Am. Sci.* 6 (2010) 353–357.
- [15] T. Akaberi, A. Shiri, S. Sheikhi-Mohammareh, Synthesis of new derivatives of pyridazino[6,1-c]pyrimido[5,4-e][1,2,4]triazine: a novel heterocyclic system, *J. Chem. Res.* 40 (2016) 44–46.
- [16] A.A. Chavan, N.R. Pai, Synthesis and biological activity of N-substituted-3-chloro-2-azetidiones, *Molecules* 12 (2007) 2467–2477.
- [17] M. Asif, Some recent approaches of biologically active substituted pyridazine and phthalazine drugs, *Curr. Med. Chem.* 19 (2012) 2984–2991.
- [18] M. Asif, A. Singh, A.A. Siddiqui, The effect of pyridazine compounds on the cardiovascular system, *Med. Chem. Res.* 21 (2012) 3336–3346.
- [19] E. Banoğlu, M. Şüküroğlu, B.Ç. Ergün, S.N. Baytaş, E. Aypar, M. Ark, Synthesis of the amide derivatives of 3-[1-(3-Pyridazinyl)-5-phenyl-1H-pyrazole-3-yl]propanoic Acids as potential analgesic compounds, *Turk. J. Chem.* 31 (2007) 677–687.
- [20] M.T. Tawfiq, Synthesis, characterization and biological activity evaluation of new pyridazines containing imidazolidine moiety, *Int. J. Adv. Res.* 4 (2015) 158–164.
- [21] J.M. Contreras, I. Parrot, W. Sippl, Y.M. Rival, C.G. Wermuth, Design, synthesis, and structure-activity relationships of a series of 3-[2-(1-benzylpiperidin-4-yl)ethylamino]pyridazine derivatives as acetylcholinesterase inhibitors, *J. Med. Chem.* 44 (2001) 2707–2718.
- [22] T.C. Ramalho, M. Rocha, E. da Cunha, M.P. Freitas, The search for new COX-2 inhibitors: a review of 2002–2008 patents, *Expert. Opin. Ther. Pat.* 19 (2009) 1–36.
- [23] A. Coelho, E. Ravina, N. Fraiz, M. Yanez, R. Laguna, E. Cano, E. Sotelo, Design, synthesis, and structure activity relationships of a novel series of 5-alkylenepyrindazin-3(2H)-ones with a non-cAMP-based antiplatelet activity, *J. Med. Chem.* 50 (2007) 6476–6484.
- [24] C. Biancanali, M.P. Giovannoni, S. Pieretti, N. Cesari, A. Graciano, C. Vergelli, A. Cilibrizzi, A. di Gianuario, M. Colucci, G. Mangano, B. Garrone, L. Polenzani, V. dal Piaz, Further studies on arylpiperazinyl alkyl pyridazinones: discovery of an exceptionally potent orally active, antinociceptive agent in thermally induced pain, *J. Med. Chem.* 52 (2009) 7397–7409.
- [25] D. Twomey, Anticancer agents–IX. Derivatives of pyridine, pyridazine and phthalazine, *Proc. R. Ir. Acad. B* 74 (1974) 4–52.
- [26] V. Pogacic, A.N. Bullock, O. Fedorov, P. Filippakopoulos, C. Gasser, A. Biondi, S. Meyer-Monard, S. Knapp, J. Schwaller, Structural analysis identifies imidazo[1,2-b]pyridazines as PIM kinase inhibitors with in vitro antileukemic activity, *Cancer Res.* 67 (2007) 6916–6924.
- [27] J. Xie, J. Bai, SGI-1776, an imidazo pyridazine compound, inhibits the proliferation of ovarian cancer cells by inactivating Pim-1, *Zhong Nan Da Xue Xue Bao Yi Xue Ban* 7 (2014) 649–657.
- [28] M.Y. Jaballah, R.T. Serya, K. Abouzid, Pyridazine based scaffolds as privileged structures in anti-Cancer therapy, *Drug Res. (Stuttg)* 3 (2017) 138–148.
- [29] A.O. Attanasi, G. Favi, P. Filippone, F.R. Perrulli, S. Santeusano, A novel and convenient protocol for synthesis of pyridazines, *Org. Lett.* 11 (2009) 309–312.
- [30] S. Lin, Z. Liu, Y. Hu, Microwave-Enhanced efficient synthesis of diversified 3,6-disubstituted pyridazines, *J. Comb. Chem.* 9 (2007) 742–744.
- [31] J.M. Wright, The double-edged sword of COX-2 selective NSAIDs, *Can. Med. Assoc. J.* 167 (2002) 1131–1137.
- [32] P. Thirusangu, V. Vigneshwaran, V.L. Ranganatha, B.R. Vijay Avin, S.A. Khanum, R. Mahmood, K. Jayashree, B.T. Prabhakar, A tumoural angiogenic gateway blocker, Benzophenone-1B represses the HIF-1 α nuclear translocation and its target gene activation against neoplastic progression, *Biochem. Pharmacol.* 125 (2017) 26–40.
- [33] H.D. Gurupadaswamy, P. Thirusangu, B.V. Avin, V. Vigneshwaran, M.P. Kumar, T.S. Abhishek, V.L. Ranganatha, S.A. Khanum, B.T. Prabhakar, DAO-9 (2,5-di(4-aryloylaryloxy)methyl)-1,3,4-oxadiazole) exhibits p53 induced apoptosis through caspase-3 mediated endonuclease activity in murine carcinoma, *Biomed. Pharmacother.* 68 (2014) 791–797.
- [34] M. Al-Ghorbani, P. Thirusangu, H.D. Gurupadaswamy, V. Girish, S.H. Neralagundi, B.T. Prabhakar, S.A. Khanum, Synthesis and antiproliferative activity of benzophenone tagged pyridine analogues towards activation of caspase activated DNase mediated nuclear fragmentation in Dalton's lymphoma, *Bioorg. Chem.* 65 (2016) 73–81.
- [35] P. Thirusangu, V. Vigneshwaran, T. Prashanth, B.V. Avin, V.H. Malojirao, H. Rakesh, S.A. Khanum, R. Mahmood, B.T. Prabhakar, BP -1T, an antiangiogenic benzophenone-thiazole pharmacophore, counteracts HIF-1 signalling through p53/MDM2-mediated HIF-1 α proteasomal degradation, *Angiogenesis* (2016) 1–17, <http://dx.doi.org/10.1007/s10456-016-9528-3>.
- [36] M.S. Zaman, V. Shahryari, G. Deng, S. Thamminana, S. Saini, M. Majid, I. Chang, H. Hirata, K. Ueno, S. Yamamura, K. Singh, Up-regulation of microRNA-21 correlates with lower kidney cancer survival, *PLoS One* 7 (2012) e31060.
- [37] J. Gu, Y. Liang, L. Qiao, Y. Lu, X. Hu, D. Luo, N. Li, L. Zhang, Y. Chen, J. Du, Q. Zheng, URI expression in cervical cancer cells is associated with higher invasion capacity and resistance to cisplatin, *Am J Cancer Res* 5 (2015) 1353–1367.
- [38] L.M. Shaw, Tumor cell invasion assays, *Methods Mol. Biol.* 294 (2005) 97–105.
- [39] E.I. Deryugina, J.P. Quigley, Matrix metalloproteinases and tumor metastasis, *Cancer Metastasis Rev.* 25 (2006) 9–34.
- [40] S.E. Gill, W.C. Parks, Metalloproteinases and their inhibitors: regulators of wound healing, *Int. J. Biochem. Cell Biol.* 40 (2008) 1334.
- [41] P. Van Lint, C. Libert, Chemokine and cytokine processing by matrix metalloproteinases and its effect on leukocyte migration and inflammation, *J. Leukoc. Biol.* 82 (2007) 1375–1381.
- [42] M. Al-Ghorbani, V. Vigneshwaran, V.L. Ranganatha, B.T. Prabhakar, S.A. Khanum, Synthesis of oxadiazole-morpholine derivatives and manifestation of the repressed CD31 Microvessel Density (MVD) as tumoral angiogenic parameters in Dalton's Lymphoma, *Bioorg. Chem.* 60 (2015) 136–146.
- [43] V.L. Ranganatha, B.V. Avin, P. Thirusangu, T. Prashanth, B.T. Prabhakar, S.A. Khanum, Synthesis, angiopreventive activity, and in vivo tumor inhibition of novel benzophenone-benzimidazole analogs, *Life Sci.* 93 (2013) 904–911.
- [44] V. Vigneshwaran, P. Thirusangu, S. Madhusudana, V. Krishna, S.N. Pramod, B.T. Prabhakar, The latex sap of the 'Old World Plant' *Lagenaria siceraria* with potent lectin activity mitigates neoplastic malignancy targeting neovasculature and cell death, *Int. Immunopharmacol.* 39 (2016) 158–171.
- [45] B.V. Avin, T. Prabhu, C.K. Ramesh, V. Vigneshwaran, M. Riaz, K. Jayashree, B.T. Prabhakar, New role of lupeol in reticence of angiogenesis, the cellular parameter of neoplastic progression in tumorigenesis models through altered gene expression, *Biochem. Biophys. Res. Commun.* 448 (2014) 139–144.
- [46] P. Thirusangu, V. Vigneshwaran, B.V. Avin, H. Rakesh, H.M. Vikas, B.T. Prabhakar, Scutellarein antagonizes the tumorigenesis by modulating cytokine VEGF mediated neoangiogenesis and DFF-40 actuated nucleosomal degradation, *Biochem. Biophys. Res. Commun.* 484 (2017) 85–92.
- [47] S.A. Amin, N. Adhikari, T. Jha, S. Gayen, First molecular modelling report on novel arylpyrimidine kynurenine monooxygenase inhibitors through multi-QSAR analysis against Huntington's disease: a proposal to chemists, *Bioorg. Med. Chem. Lett.* 26 (2016) 5712–5718.
- [48] S.A. Amin, S. Bhargava, N. Adhikari, S. Gayen, T. Jha, Exploring pyrazolo[3,4-d]pyrimidine phosphodiesterase 1 (PDE1) inhibitors: a predictive approach combining comparative validated multiple molecular modelling techniques, *J. Biomol. Struct. Dyn.* (2017), <http://dx.doi.org/10.1080/07391102.2017.1288659>.